Optics and Lasers in Engineering 134 (2020) 106273

Contents lists available at ScienceDirect

Optics and Lasers in Engineering

journal homepage: www.elsevier.com/locate/optlaseng

Fabrication of homogenous subwavelength grating structures on metallic glass using double-pulsed femtosecond lasers

Yuhao Lei [a,b], Jianjun Yang [a,b,*], Cong Cong [c], Chunlei Guo [b,c]

[a] Institute of Modern Optics, Nankai University, Tianjin 300350, China
[b] The Guo China-US Photonics Laboratory, State Key Laboratory of Applied Optics, Changchun Institute of Optics, Fine Mechanics and Physics, Chinese Academy of Sciences, Changchun 130033, China
[c] The Institute of Optics, University of Rochester, Rochester, NY, 14627, USA

ARTICLE INFO

Keywords:
Femtosecond laser
Laser-induced periodic surface structures
Metallic glass

ABSTRACT

We report a formation of highly homogenous subwavelength grating structures on the bulk Fe-based metallic glass, using two nondegenerate linear polarization of femtosecond laser pulse sequences at certain temporal delays. In contrast to the previous observations, the well-defined surface structures can take place across the entire laser ablation regions, with the spatial period and the modulation depth of 722 nm and 115 nm, respectively. Through the Fourier transformation analysis, we introduce two parameters to quantitatively evaluate the structure uniformity. The underlying mechanisms are attributed to the surface scattered wave of the second femtosecond laser pulse onto the transient material surface tailored by the first laser pulse. Moreover, different diffusion coefficients of the chemical elements are found responsible for their various removal percentages after laser irradiation.

1. Introduction

As a universal phenomenon of laser-solid interaction, laser-induced periodic surface structures have been studied extensively for several decades since the first discovery by Birnbaum on semiconductor surface [1]. With the availability of femtosecond laser pulses [2], this research has gained an increasing attraction and promoted the structure accuracy into a regime of subwavelength or deep-subwavelength scales [3–5]. Now we can understand that such direct formation of the periodic structures in a single-step process not only includes the abundant physics, but also re-functionalize materials via a control of optical [6,7], mechanical [8,9], or chemical [10] surface properties. For the bulk materials, however, most of the previous studies demonstrated that the laser-induced surface structures (or ripples) often present the ablative characteristics with irregular or semi-periodic profiles [11–14]. The formation mechanisms of the subwavelength ripples were usually ascribed to interference of the incident laser and its excited surface plasmons [15]. Besides, the pump-probe imaging approach is able to reveal the formation dynamics of ripples from picosecond to nanosecond scales [16,17]. The spatial irregularity of the ripple structures maybe due to the tight focusing of the Gaussian laser beam intensity and complex feedbacks of the surface defects to the scattered light [18,19]. With the help of cylindrical focusing conditions to make slowly varying intensity distribution in the central part of the laser beam spot, a large area of the regular subwavelength ripple structures has been induced on a dielectric surface [14]. On the other hand, through adopting film materials, Öktem et.al. reported the uniform formation non-ablative grating structures with bulging-like profiles on titanium (Ti) thin film of due to the oxidation process [20]. Moreover, the fabrication of highly regular ripple structures have been also demonstrated on molybdenum (Mo) film with 300 nm thickness via a f-theta lens focused femtosecond laser beam [21]. In contrast to thin films, bulk metallic materials have wider applications in industry and research because of the advantages such as hardness and durability, and undoubtedly, their usage values can be further improved by the nanomanipulation of surface. Recently, the highly uniform ripple structures have been demonstrated on Zr metallic glass using the single pulse sequences of femtosecond laser [22,23]. However, how to generate the high-quality subwavelength structures in a long range on bulk metal materials remains an open question for femtosecond laser precision manufacturing.

In this paper, we report the fabrication of the ultra-uniform subwavelength grating structures on a bulk Fe-based metallic glass ($Fe_{82}Si_{11}C_7$), by using two temporally delayed femtosecond laser pulse sequences with different linear polarizations. Laser spatial intensity distribution was modified by a hard aperture. The high quality of the surface structures can be properly maintained in the whole laser ablation region,

* Corresponding author at: The Guo China-US Photonics Laboratory, State Key Laboratory of Applied Optics, Changchun Institute of Optics, Fine Mechanics and Physics, Chinese Academy of Sciences, Changchun 130033, China.
E-mail address: jjyang@ciomp.ac.cn (J. Yang).

https://doi.org/10.1016/j.optlaseng.2020.106273
Received 22 December 2019; Received in revised form 4 June 2020; Accepted 9 June 2020
Available online 18 June 2020

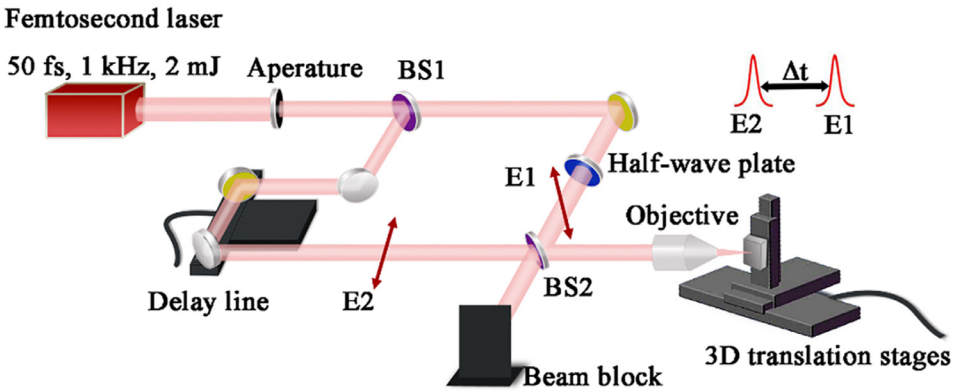

Fig. 1. Diagram of the experimental setup for the formation of the ultra-uniform subwavelength structures on Fe-based metallic glass using two controllable time-delayed femtosecond laser pulse sequences. E1 and E2 represent directions of the linear polarization of two femtosecond laser pulses, respectively.

which can also be extended in the laser scanning direction. This method is mask-free and requires no further chemical etching process. Besides the traditional morphologic examinations, the structure uniformity is comprehensively analyzed via a two-dimensional fast Fourier transformation (2D-FFT) process. The obtained results demonstrate the time delay effects on the improving uniformity, and finally the underlying mechanisms are discussed. Furthermore, the spatially selective modification of the chemical elements is also investigated.

2. Materials and methods

A schematic diagram of the experiment is shown in Fig. 1, where a commercial Ti:sapphire laser amplifier was employed as the light source, which delivers the horizontally polarized femtosecond laser at the repetition rate of 1 kHz, with the time duration of 50 fs and the central wavelength of 800 nm, respectively. A beam diameter of the laser pulses out of the amplifier is 8 mm. Before splitting the laser pulse into two pulses by a beam splitter (BS1), a 3.2 mm diameter of hard aperture was used for modifying the spatial profile of the laser intensity [24,25]. After passing an optical delay line, the double pulse sequence were provided with a temporal separation Δt and then spatially overlapped for a collinear propagation. Moreover, in one optical path we inserted a half wave-plate to rotate the direction of the linear polarization of the laser pulse (E1) by 45° with respect to that of another laser pulse (E2) (which keeps the horizontal polarization). An objective lens (4 ×, N.A.=0.1) was used for focusing the two femtosecond lasers onto the metallic glass surface at normal incidence. A three-dimensional translation stage (Newport, ESP301) was used to precisely control the scanning speed and the sample position. The sample surface was placed 500 μm before the laser focus and the calculated diameter of laser spot was around 100 μm. The experiment was carried out in ambient air by a line-scribing method with a scanning speed of 1 mm/s, resulting in approximate 100 laser pulses partially overlapped in a beam spot area. The experimentally measured single pulse ablation threshold fluence for this material was about 0.23 J/cm^2.

The selection of Fe-based metallic glass was based on its superior physical and chemical properties, such as soft magnetic properties, excellent corrosion resistance and super-high hardness [26,27]. The surface morphologies of laser-irradiated regions were characterized by scanning electron microscopy (SEM, Keyence, VE-9800) and atomic force microscopy (AFM, Bruker, D8 Focus). No surface preparation including ultrasonic cleaning or chemical etching was carried out before SEM and AFM imaging. The elements distribution were measured by energy-dispersive X-ray spectroscopy (EDS, Phenom, ProX).

3. Results and discussions

In our experiments, the intersection angle between directions of two laser polarizations is 45 °. As shown in Fig. 2, when the two femtosecond laser pulse sequences (with the same energy fluence of 0.02 J/cm^2) stroke the target at different time delays (the horizontally polarized laser E2 was delayed), the one-dimensional (1D) subwavelength periodic structures was formed on Fe-based metallic glass surface. However, with varying time delay between two laser pulses, the appearance of the constructed structures seems to be different. For example, at the time delays of $\Delta t = 0$ ps, 10 ps, and 20 ps, [Fig. 2(a-c)] the achieved grating-like structures can be found splitting phenomenon on the ridges, which makes the spatial regularity not so well. In contrast, when the time delay increased from $\Delta t = 30$ ps to 70 ps [Fig. 2 (d-h)] the uniformity of the structure morphology becomes more desirable. Furthermore, the spatial orientation of the grating-like structures appears to change at different time delays between double laser pulses. More specifically, the ripple orientations at the inter-pulse time delays of $\Delta t = 60$ ps and 70 ps can be evidently different. It is well known that for the irradiation of single pulse sequences, the available ripple orientation is usually either perpendicular or horizontal to the direction of the laser polarization. However, under irradiation of double pulse sequences, the spatial orientation of the achieved ripple structures is not only dominated by the laser polarization, but also affected by the inter-pulse time delay. Such phenomena could be attributed to the ripple formation process from the surface wave excitation of the delayed pulse on the transient-state of the material surface modulated by the incident first one of double pair pulses [28].

Fig. 3(a) shows a typical result at the time delay of $\Delta t = 58$ ps, where 1D subwavelength grating- structures present two striking features: one is their extraordinarily uniform distribution on the whole laser ablated region, without disintegrated irregularities such as bend, breaking and bifurcation. In addition, the regular arrangement along the scanning direction indicates the robust extension of such structures during the sample translation; the other is the structure orientation perpendicular to the direction of the linear polarization of the delayed laser pulse E2. Remarkably, through comparing the center part and the periphery of the laser scanned areas, we can find that the structure uniformity can take place across the entire laser ablated spot area in spite of the incident Gaussian laser intensity, in sharp contrast to the observations in most previous studies [29,30]. The corresponding high-resolution SEM images, as shown in Fig. 3(b) and (c), reveal that the ablated periodic grooves have only 140 nm in width, with unusually sharp and straight appearance. In addition, the measured structure period of 722 nm is less than the incident laser wavelength.

For comparison, Fig. 3(d) demonstrates the obtained result using a single pulse sequence femtosecond laser (with the energy fluence of 0.02 J/cm^2). Clearly, the laser-exposed surface was also modified into 1D grating-like structures, with orientation perpendicular to the direction of the incident laser polarization. The measured spatial period was 745 ± 25 nm. This observation is very similar to the previous reports on other materials [9]. The detailed inspects reveal the ridge-splitting and irregular bending phenomena, as shown in Fig. 3(e), which of course degrades the spatial regularity of the surface structures.

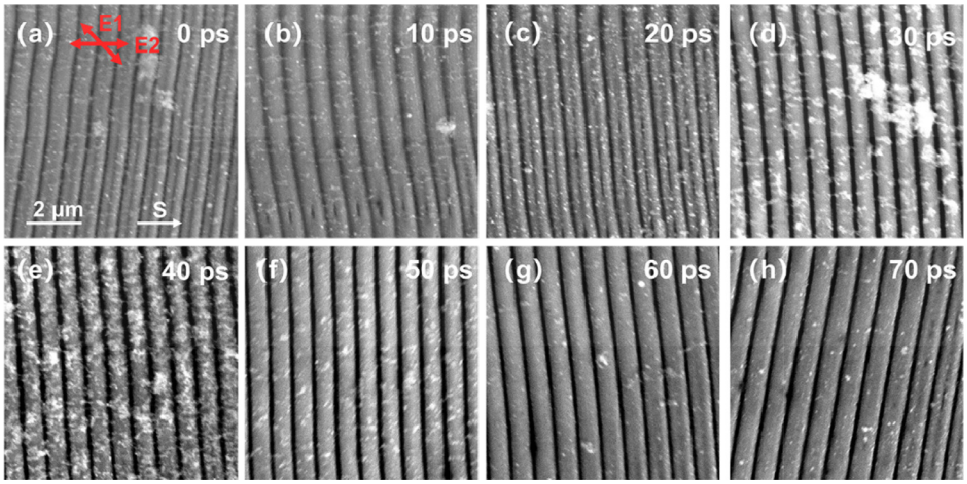

Fig. 2. SEM images of subwavelength-scaled surface structures formed on the Fe-based metallic glass by two femtosecond laser pulse sequences with different time delays between two pulses: (a-h) Δt = 0–70 ps. The intersection angle between directions of two laser polarizations (E1 and E2) is fixed at 45°; the energy fluence of each laser pulse is the same of 0.02 J/cm^2.S represents the direction of the sample scanning.

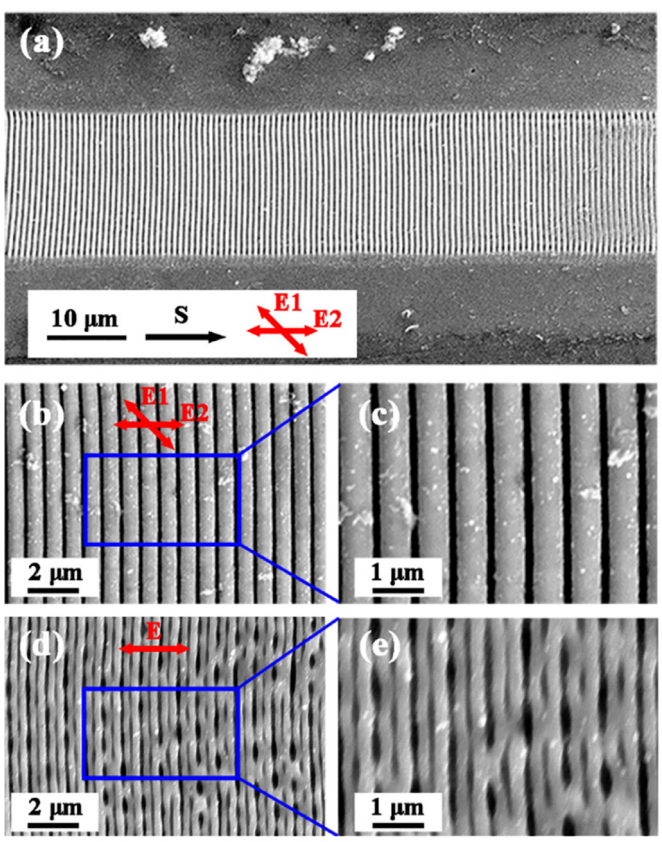

Fig. 3. Constructing the subwavelength-scaled surface structures on the Fe-based metallic glass by two femtosecond laser pulse sequences. (a) Ultra-uniform surface structures over a long-range scanning area induced by two femtosecond laser pulse sequences at the time delay of Δt = 58 ps, with the intersection angle of 45° between the two laser polarizations (E1 and E2). (b) and (c) are the magnified views of (a). (d) Semi-periodic surface structures with ripple splitting induced by a single pulse sequence femtosecond laser, with E denoting the direction of the laser polarization. (e) is the enlarged image of (d). The energy fluence of each laser pulse in both (a) and (d) is to the same of 0.02 J/cm^2, and S represents the direction of laser scanning.

In fact, a deep analysis of the uniformity of the whole structures can be achieved in the frequency domain through 2D-FFT [14,21], and Fig. 4(a) is a transformation image of Fig. 3(a). From this process, we can obtain two evaluation parameters: the period uncertainty and the orientation uncertainty. Because each peak value in the Fourier frequency domain is usually written by two components: $f_x = \overline{f_x} \pm \Delta f_x$ and $f_y = \overline{f_y} \pm \Delta f_y$, as shown in Fig. 4(b), the retrieved structure period of 722 ± 9 nm can be obtained from the fundamental spatial frequencies (f_x and f_y) by a formula of $\Lambda = \frac{1}{f} = \frac{1}{\sqrt{f_x^2+f_y^2}}$, which is in good agreement with the measured data in the spatial domain. The period uncertainty, $\Delta\Lambda/\Lambda$, can be calculated from the full-width-at-half-maximum (FWHM) intensity values of the fundamental frequencies in two components, Δf_x and Δf_y, where

$$\Delta\Lambda \approx |d\Lambda| = \left|d\left(\frac{1}{\sqrt{f_x^2+f_y^2}}\right)\right| = \left|\left(-\frac{1}{2}\right)\frac{2f_x\,df_x + 2f_y\,df_y}{\left(f_x^2+f_y^2\right)^{\frac{3}{2}}}\right| = \frac{\sqrt{\overline{f_x}^2\Delta f_x^2 + \overline{f_y}^2\Delta f_y^2}}{\left(\overline{f_x}^2+\overline{f_y}^2\right)^{\frac{3}{2}}} \quad (1)$$

Similarly, the orientation uncertainty of the structures is defined by $\frac{\Delta\theta}{\theta}$, from the Fourier frequency domain, where $\theta = \arctan\frac{f_x}{f_y}$, and

$$\triangle\theta \approx |d\theta| = \left|d\left(arctan\left(\frac{f_x}{f_y}\right)\right)\right| = \left|\frac{d\left(\frac{f_x}{f_y}\right)}{\frac{f_x^2}{f_y^2}+1}\right| = \left|\frac{f_x df_y - f_y df_x}{f_x^2+f_y^2}\right| = \frac{\sqrt{\overline{f}_x^2\triangle f_y^2 + \overline{f}_y^2\triangle f_x^2}}{\overline{f}_x^2+\overline{f}_y^2}. \quad (2)$$

Based on the above method, we obtained the evolution of two evaluation parameters for the structure formation within the time-delay range of Δt = 0~80 ps, as demonstrated in Fig. 4(c)-(d). Clearly, the time-delay dependent variations of the two parameters exhibit the very similar tendency, i.e., the obtained larger values usually appear within a range of $\Delta t < 30$ ps, while the achieved smaller values, indicating the enhanced uniformity for the subwavelength structure formation, emerge at the time delays around Δt=50~60 ps. Generally, when compared with the calculation results of the single pulse sequence laser irradiation, as shown by dashed lines, the double-laser induced subwavelength surface structures can present the higher quality at the proper time delays.

Fig. 5 shows the AFM measurement results of the surface structures obtained at the time delay of Δt = 58 ps, whose quantitative description of the modulation depth is 115 nm. In particular, the achieved cross-section curves at three different positions (marked by different color

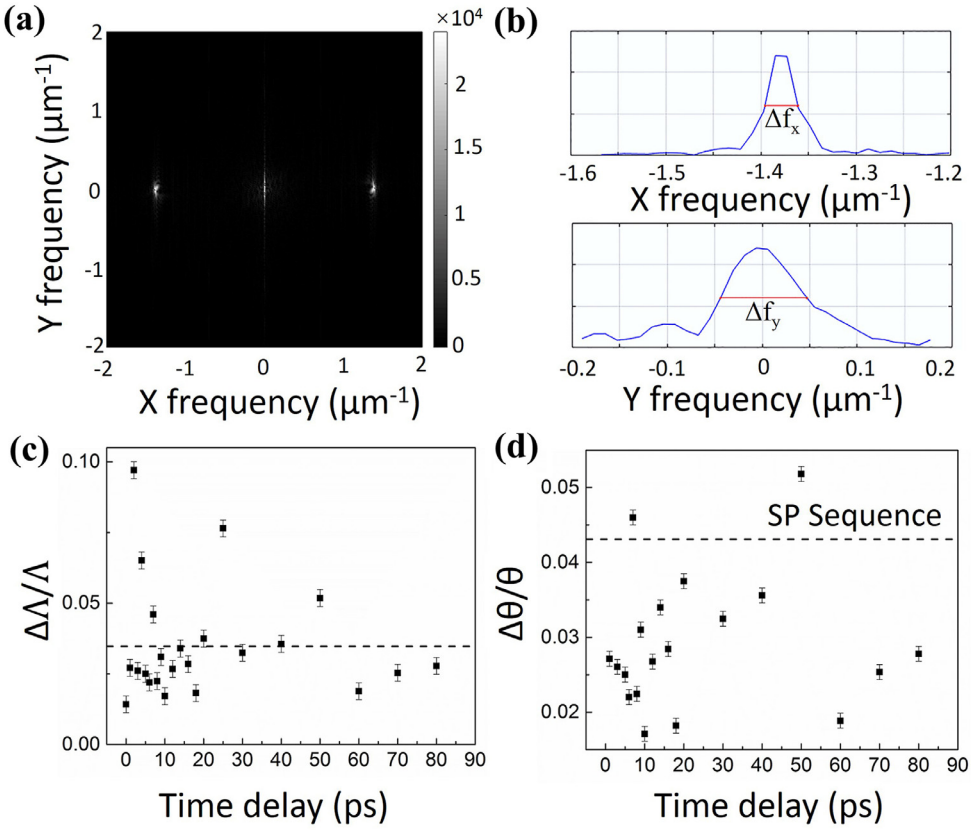

Fig. 4. (a) 2D-FFT image of Fig. 3(a); (b) Δf_x and Δf_y; (c-d) are the obtained two parameters (the period uncertainty and the orientation uncertainty, respectively) through FFT method for characterizing the structure uniformity as a function of the time delay between two lasers. The black squares denote the double-pulsed femtosecond laser irradiation, and the dashed lines represent situations of the single pulse (SP) sequence irradiation.

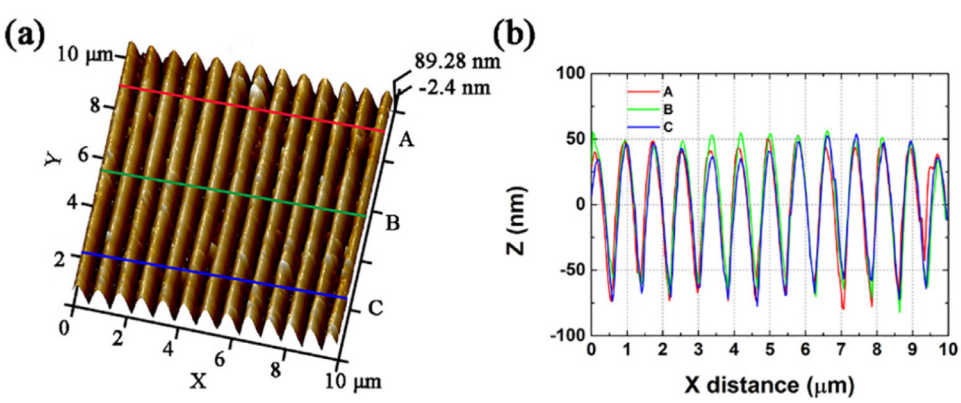

Fig. 5. AFM measurement results of the laser-induced uniform surface structures on Fe-based metallic glass. (a) Three-dimensional image. (b) Cross-section profiles along three different lines marked in (a).

lines) exhibit a remarkable consistency (the fractional variations may be due to the deposition of debris), which confirms the good spatial uniformity of the laser-induced surface structures. Fig. 6 presents the measured EDS mappings on the surface structures, which reveal that after the laser treatment the spatial distribution of three chemical elements of Fe, Si and C, would like to show the periodic patterns, which are in good consistent with the corresponding surface morphology. It is clear that the colored region represents the element rich place and the white region for element poor area. However, the strength of the periodic variation appears to depend on the chemical elements, i.e., for the elements of Fe and Si, the periodic change tendencies in the EDS maps are indistinct, whereas the spatial distribution of the element C presents the pronounced periodic tendency, which indicates the larger percentage of the element removal.

The underlying mechanisms for the formation of such highly uniform subwavelength surface structures can be attributed to the following factors: (i) the absence of an ordered atomic-scale structure, crystallites, grain boundaries, and dislocations in the amorphous state of Fe-based metallic glass [31]. (ii) the Fe-based metallic glass has high plasticity and ductility, which makes the material not easy break under thermoplastic forming after the laser irradiation [32,33]. (iii) The transient decrease of surface roughness by the larger mobility of atoms due to the thermal heating of the first laser pulse [34,35]. (iv) the flattening of spatial intensity distribution of the laser by the hard aperture [24,25]. Therefore, the intensity fringes caused by interference between the incident second laser pulse and scattered surface wave become homogeneously distributed on the material surface [15,18]. Alternatively, the morphologic traces induced by the first laser pulse on the sample surface would like to be washed out by the time-delayed femtosecond laser pulse, resulting in the spatial orientation of the periodic structures perpendicular to the direction of the polarization of the second laser [$\Delta t = 58$ ps]. Moreover, compared with the single pulse sequence laser irradiation, the negligible morphology splitting of the surface structures induced by the double pulse sequences may be due to the change in the

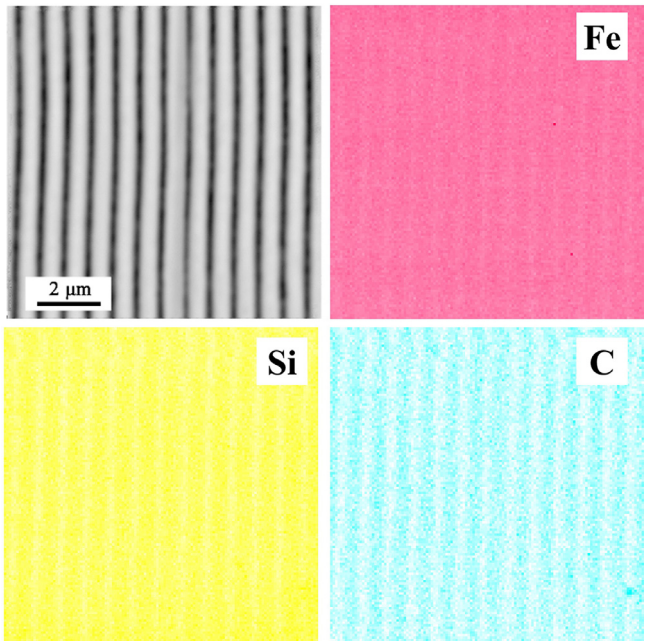

Fig. 6. SEM image and mapping of the periodic distribution of three chemical elements (Fe, Si and C) by energy dispersive spectroscopy.

modulation depth of the structures [36,37], when thermal softening of the material surface caused by the first laser is considered. On the other hand, X-ray diffraction measurement confirmed that no crystallization happens for the metallic glass under irradiation of such low laser fluence [29]. In addition, we conclude that the reason why three chemical elements show the spatially periodic distribution patterns is that the laser-induced temperature gradient on the surface followed by the periodic material removal [38]. Because the diffusion coefficient of the element carbon ($\sim 10^{-7}$ cm^2/s) is the highest in metallic glass compared with the elements silicon ($\sim 10^{-8}$ cm^2/s) and iron ($\sim 10^{-10}$ cm^2/s) [39,40], the removal percentage of carbon is the largest in these three chemical elements. Another explanation for various removal percentages of three elements is the selective vaporization due to their different thermal properties [19,41]. However, the amorphous phase of the sample is unchanged after laser irradiation [35].

4. Conclusion

To summarize, we have successfully presented a strategy that allows us to obtain the highly ordered grating structures on the bulk Fe-based metallic glass, upon irradiation of time-delayed double femtosecond lasers (1 kHz, 800 nm and 50 fs) with nondegenerate directions of the linear polarizations. Morphological examinations reveal the highly homogenous structure formation across the entire laser ablated area, which can be even robustly extended along the scanning direction. Moreover, a comprehensive evaluation of the structural uniformity is achieved by the introduction of two factors via the Fourier transformation process. The physical reasons are attributed to both the amorphous state of the sample and the further surface smoothening by irradiation of the first femtosecond laser pulse sequence. These results enable potential values in the high-quality femtosecond laser micro processing of metal surfaces for many promising applications.

Declaration of Competing Interest

The authors declare that they have no known competing financial interests or personal relationships that could have appeared to influence the work reported in this paper.

Author statement

Y.L. and J.Y. conceived and designed the experiments; Y.L. performed the experiments; C.C. and Y.L. performed the mathematical analysis; Y. L., C.C. and J.J analyzed the data; Y.L., J.Y., and C.G. wrote and revised the paper. All the authors commented on the paper. J.Y. and C. G. supervised the project.

Acknowledgments

This work is financially supported by National Natural Science Foundation of China (91750205, 11674178); Jilin Provincial Science & Technology Development Project (20180414019GH); Strategic Priority Research Program of Chinese Academy of Sciences (XDA22010302); K. C. Wong Education Foundation (GJTD-2018-08). The authors appreciate Dr. Joshya Shyamala Rojogapal and Dr. Chi Vinh Ngo for the critical reading.

References

[1] Birnbaum M. Semiconductor surface damage produced by ruby lasers. J Appl Phys 1965;36(11):3688–9.
[2] Strickland D, Mourou G. Compression of amplified chirped optical pulses. Opt Commun 1985;56(3):219–21.
[3] Vorobyev AY, Guo C. Direct femtosecond laser surface nano/microstructuring and its applications. Laser Photonics Rev 2013;7(3):385–407.
[4] Bonse J, Höhm S, Kirner SV, Rosenfeld A, Krüger J. Laser-induced periodic surface structures—a scientific evergreen. IEEE J Sel Top Quantum Electron 2017;23(3):1–15.
[5] Reif J, Costache F, Henyk M, Pandelov SV. Ripples revisited: non-classical morphology at the bottom of femtosecond laser ablation craters in transparent dielectrics. Appl Surf Sci 2002;197-198:891–5.
[6] Vorobyev AY, Guo C. Colorizing metals with femtosecond laser pulses. Appl Phys Lett 2008;92(4):041914.
[7] Vorobyev AY, Guo C. Direct creation of black silicon using femtosecond laser pulses. Appl Surf Sci 2011;257(16):7291–4.
[8] Athanasiou CE, Hongler MO, Bellouard Y. Unraveling brittle-fracture statistics from intermittent patterns formed during femtosecond laser exposure. Phys Rev Appl 2017;8(5):54013.
[9] Bonse J, Koter R, Hartelt M, Spaltmann D, Pentzien S, Höhm S, Rosenfeld A, Krüger J. Femtosecond laser-induced periodic surface structures on steel and titanium alloy for tribological applications. Appl Phys A 2014;117(1):103–10.
[10] Vorobyev AY, Guo C. Laser turns silicon superwicking. Opt Express 2010;18(7):6455–60.
[11] Bonse J, Baudach S, Krüger J, Kautek W, Lenzner M. Femtosecond laser ablation of silicon–modification thresholds and morphology. Appl Phys A 2002;74(1):19–25.
[12] Ruiz de la Cruz A, Lahoz R, Siegel J, de la Fuente GF, Solis J. High speed inscription of uniform, large-area laser-induced periodic surface structures in Cr films using a high repetition rate fs laser. Opt Lett 2014;39(8):2491–4.
[13] Yang Y, Yang J, Xue L, Guo Y. Surface patterning on periodicity of femtosecond laser-induced ripples. Appl Phys Lett 2010;97(14):141101.
[14] Wang L, Chen QD, Cao XW, Buividas R, Wang X, Juodkazis S, Sun HB. Plasmonic nano-printing: large-area nanoscale energy deposition for efficient surface texturing. Light Sci Appl 2017;6(12):e17112.
[15] Huang M, Zhao F, Cheng Y, Xu N, Xu Z. Origin of laser-induced near-subwavelength ripples: interference between surface plasmons and incident laser. ACS Nano 2009;3(12):4062–70.
[16] Jia X, Jia TQ, Peng NN, Feng DH, Zhang SA, Sun ZR. Dynamics of femtosecond laser-induced periodic surface structures on silicon by high spatial and temporal resolution imaging. J Appl Phys 2014;115(14):143102.
[17] Garcia-Lechuga M, Puerto D, Fuentes-Edfuf Y, Solis J, Siegel J. Ultrafast moving-spot microscopy: birth and growth of laser-induced periodic surface structures. ACS Photonics 2016;3(10):1961–7.
[18] Sipe JE, Young JF, Preston JS, van Driel HM. Laser-induced periodic surface structure. I. Theory. Phys Rev B 1983;27(2):1141–54.
[19] Li C, Zhang H, Cheng G, Faure N, Jamon D, Colombier J-P, et al. Initial cumulative effects in femtosecond pulsed laser-induced periodic surface structures on bulk metallic glasses. J Laser Micro Nanoen 2016;11(3):357–65.
[20] Öktem B, Pavlov I, Ilday S, Kalaycıoğlu H, Rybak A, Yavaş S, Erdoğan M, Ilday FÖ. Nonlinear laser lithography for indefinitely large-area nanostructuring with femtosecond pulses. Nat Photonics 2013;7(11):897–901.
[21] Gnilitskyi I, Derrien TJ, Levy Y, Bulgakova NM, Mocek T, Orazi L. High-speed manufacturing of highly regular femtosecond laser-induced periodic surface structures: physical origin of regularity. Sci Rep 2017;7(1):8485.
[22] Li C, Cheng G, Sedao X, Zhang W, Zhang H, Faure N, Jamon D, Colombier J-P, Stoian R. Scattering effects and high-spatial-frequency nanostructures on ultrafast laser irradiated surfaces of zirconium metallic alloys with nano-scaled topographies. Opt Express 2016;24(11):11558–68.
[23] Zhang W, Cheng G, Hui X, Feng Q. Abnormal ripple patterns with enhanced regularity and continuity in a bulk metallic glass induced by femtosecond laser irradiation. Appl Phys A 2014;115(4):1451–5.

[24] Dumitru G, Romano V, Weber HP, Sentis M, Marine W. Femtosecond ablation of ultrahard materials. Appl Phys A 2002;74(6):729–39.
[25] Liao Y, Shen Y, Qiao L, Chen D, Cheng Y, Sugioka K, Midorikawa K. Femtosecond laser nanostructuring in porous glass with sub-50nm feature sizes. Opt Lett 2013;38(2):187–9.
[26] Yavari AR, Lewandowski JJ, Eckert J. Mechanical properties of bulk metallic glasses. MRS Bull 2007;32(8):635–8.
[27] Gu XJ, Poon SJ, Shiflet GJ. Mechanical properties of iron-based bulk metallic glasses. J Mater Res 2011;22(02):344–51.
[28] He W, Yang J. Probing ultrafast nonequilibrium dynamics in single-crystal SiC through surface nanostructures induced by femtosecond laser pulses. J App Phys 2017;121(12):123108.
[29] Wang J, Guo C. Ultrafast dynamics of femtosecond laser-induced periodic surface pattern formation on metals. Appl Phys Lett 2005;87(25):251914.
[30] Bonse J, Krüger J. Pulse number dependence of laser-induced periodic surface structures for femtosecond laser irradiation of silicon. J App Phys 2010;108(3):034903.
[31] Greer AL. Metallic glasses. Science 1995;267(5206):1947–53.
[32] Schroers J. Processing of bulk metallic glass. Adv Mater 2010;22(14):1566–97.
[33] Yang W, Liu H, Zhao Y, Inoue A, Jiang K, Huo J, Ling H, Li Q, Shen B. Mechanical properties and structural features of novel Fe-based bulk metallic glasses with unprecedented plasticity. Sci Rep 2014;4:6233.
[34] Cao CR, Lu YM, Bai HY, Wang WH. High surface mobility and fast surface enhanced crystallization of metallic glass. Appl Phys Lett 2015;107(14):141606.
[35] Lei Y, Zhang N, Yang J, Guo C. Femtosecond laser eraser for controllable removing periodic microstructures on Fe-based metallic glass surfaces. Opt Express 2018;26(5):5102.
[36] Huang M, Cheng Y, Zhao F, Xu Z. The significant role of plasmonic effects in femtosecond laser-induced grating fabrication on the nanoscale. Ann Phys 2013;525(1–2):74–86.
[37] Hou S, Huo Y, Xiong P, Zhang Y, Zhang S, Jia T, Sun Z, Qiu J, Xu Z. Formation of long- and short-periodic nanoripples on stainless steel irradiated by femtosecond laser pulses. J Phys D Appl Phys 2011;44(50):505401.
[38] Sakakura M, Shimizu M, Shimotsuma Y, Miura K, Hirao K. Temperature distribution and modification mechanism inside glass with heat accumulation during 250kHz irradiation of femtosecond laser pulses. Appl Phys Lett 2008;93(23):231112.
[39] Borg RJ, Lai DYF. Diffusion in α-Fe–Si alloys. J App Phys 1970;41(13):5193–200.
[40] Tibbetts GG. Diffusivity of carbon in iron and steels at high temperatures. J App Phys 1980;51(9):4813–16.
[41] Shimizu M, Sakakura M, Kanehira S, Nishi M, Shimotsuma Y, Hirao K, Miura K. Formation mechanism of element distribution in glass under femtosecond laser irradiation. Opt Lett 2011;36(11):2161–3.